Recent Advances in Muffler Acoustics

M. L. Munjal

Facility for Research in Technical Acoustics (FRITA), Department of Mechanical Engineering, Indian Institute of Science, Bangalore — 560 012, India.

(Received 23 December 2011; Accepted 14 November 2012)

Exhaust noise in engines has always been a major source of automotive noise. Challenges for muffler design have been constraints on size, back pressure, and, of course, the cost. Designing for sufficient insertion loss at the engine firing frequency and the first few harmonics has been the biggest challenge. Most advances in the design of efficient mufflers have resulted from linear plane wave theory, making use of the transfer matrix method. This review paper deals with evaluating approximate source characteristics required for prediction of the unmuffled intake and exhaust noise, making use of the electroacoustical analogies. In the last few years, significant advances have been made in the analysis of variable area perforated ducts, transverse plane wave analysis of short elliptical as well as circular chambers, double-tuned expansion chambers and concentric tube resonators, catalytic converters, diesel particulate filters, air cleaners, etc. The development of long strand fibrous materials that can be used in hot exhaust systems without binders has led to the use of combination mufflers in exhaust systems. Breakthroughs have been achieved in the prediction and control of breakout noise from the elliptical and circular muffler shell as well as the end plates of typical mufflers. Diesel particulate filters and inlet air cleaners have also been modeled acoustically. Some of these recent advances are the subject of this review paper.

1. INTRODUCTION

Mufflers are essentially low-pass acoustical filters. Making use of electroacoustical analogies,[1] lumped inductance and capacitance of electrical wave filter are represented in mufflers by connecting pipes (or ducts) and chambers (or plenums), respectively. Helmholtz resonators of musical acoustics have also found their counterpart here in the form of a hole-cavity resonator. Although the science of acoustics of ducts and mufflers is over 150 years old,[2] the first comprehensive experimental investigation on analysis and design of mufflers for internal combustion engines was reported by Davis et al. in 1954.[3] The classical 1-D or plane wave theory with progressive waves moving in either direction led to the development of the transfer matrix method (TMM), which is ideally suited for acoustical modelling of cascaded elements constituting typical automotive mufflers.[4]

The TMM makes use of the standing wave variables to move from one element to the next in the cascade. Computationally, successive multiplication of transfer matrices is much faster as well as more convenient than formulation and simultaneous solution of a large number of linear algebraic equations. In fact, a heuristic study of the transfer matrix multiplication process led to the development of a user-friendly algebraic algorithm,[5] which in turn helped in a rational synthesis of 1-D acoustical filters[6] as well as vibration isolators.[7]

Morfey's work on the sound generation and propagation in ducts with mean flow[8] indicated that the convective effect of mean flow[9] is to augment the flow-acoustical power of the forward wave and reduce that of the rearward (or reflected) wave. This led to the definition of convective (or flow acoustical) state variables (p_c, v_c) that are linearly related in the classical (stationary medium) state variables (p, v). Replacement of (p, v) with (p_c, v_c) yields identically similar expressions for insertion loss (IL) of a muffler with incompressible mean flow.[10] The transformation relations between (p, v) and (p_c, v_c) enable conversion of the transfer matrices in classical state variables with a moving medium to their counterparts in convective state variables and vice versa.

A Helmholtz resonator introduces a sharp peak at its resonance frequency.[10] However, designing an automotive muffler requires wide-band domes. Therefore, a designer would use pipes with extended perforations opening into an annular cavity. The resulting concentric tube resonator was first modelled by Sullivan and Crocker,[11] making use of a 1-D control volume approach. The resulting coupled equations were solved by writing the acoustical field in the annular cylindrical cavity as a summation of natural modes satisfying the rigid-wall boundary conditions at the two ends. Sullivan followed it up with a segmentation approach which was applicable to a configuration with even three interacting ducts.[12] Munjal, Narayana Rao, and Sahasrabudhe developed a generalized decoupling approach for such perforated-element configurations.[13,14] This approach was soon followed by Peat's eigenvalue analysis,[15] which was particularly tailored for digital computation, where we can make use of the standard subroutines or library functions. A parametric study by Munjal, Krishnan, and Reddy yielded a relative flow-acoustical performance of concentric tube resonators, plug mufflers, and chambers with three interacting ducts.[16] Empirical expressions for the stagnation pressure drop for all three types of perforated-element muffler configurations were derived in terms of the open-area ratio of the perforate.[16]

Over the next decade, a large amount of research was reported on acoustical analysis of complex perforated elements,[17–24] particularly the open-end flow-reversal elements[24] and acoustical characterization of the exhaust and intake system of the reciprocating internal combustion engines.

Automobile engine is a variable speed engine, and therefore, a muffler must act as a low-pass filter with adequate wide-

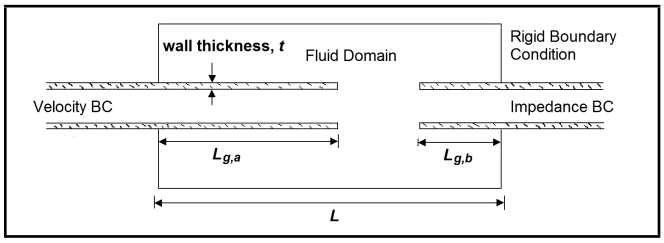

Figure 1. Geometry of the fluid domain incorporating wall thickness and boundary conditions.[27]

band IL. Starting from the firing frequency corresponding to the idling speed of the engine, dips, if any, in the transmission loss (TL; or IL) curve may severely compromise the overall IL of the muffler, owing to the implications of the anti-logarithmic addition of sound pressure levels (SPL). Most of the unmuffled exhaust noise is associated with the first few (say, 10) speed orders of the engine, and therefore, the plane wave or 1-D analysis of the muffler would do.[14] For large mufflers and/or at higher frequencies, higher-order modes would start propagating unattenuated, and then a rigorous 3-D analysis may be necessary. Besides, breakout noise from the muffler shell and end plate would limit the net IL. This paper reviews the relatively recent advances in the following areas:

(1) double-tuned expansion chambers,

(2) tuning of the extended concentric tube resonators,

(3) transverse plane-wave analysis of end chambers,

(4) source characterization of the engine,

(5) multiply-connected mufflers,

(6) breakout noise from the muffler shell and end plates,

1.](7)] diesel particulate filters and inlet air cleaners.

In this review paper, there is an unavoidable bias towards the research work of the author and his former students and associates. Nevertheless, reference has been made to the salient contributions of contemporary researchers worldwide.

2. DOUBLE-TUNED EXPANSION CHAMBERS

The TL spectrum of a simple expansion chamber is characterized by periodic peaks and troughs. The peak of the TL lobe depends on the expansion area of the simple expansion chamber and width of the lobe depends upon the length of the chamber. The chamber length troughs occur at $kL = m\pi$, $m = 0, 1, 2, 3, \ldots$.

According to the 1-D plane wave theory, the peaks of TL of the extended inlet elements (see Fig. 1) occur at resonance frequencies given by[14]

$$-jY\cot(kL_a) = 0. \tag{1}$$

If the length of the extended inlet element $L_a = L/2$, then the resonance peaks would occur at

$$kL = (2n-1)\pi; \qquad n = 1, 2, 3, \ldots; \tag{2}$$

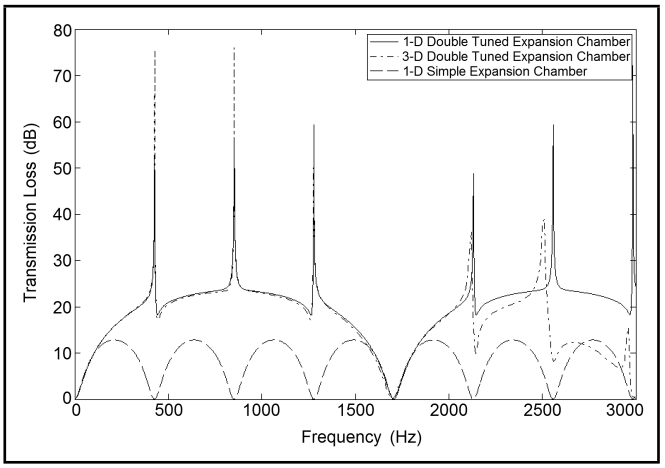

Figure 2. Comparison between the 1-D and 3-D models for the configuration of Fig. 1, with end corrections applied to the 1-D model.[27] ($L_{g,a} = 189.1$ mm, $L_{g,b} = 87.4$ mm, $L_a = 203.25$ mm, $L_b = 101.625$ mm, $\delta_a = 14.1$ mm, $\delta_b = 14.25$ mm, and $L = 406.5$ mm).

where L is total length of the expansion chamber, L_a is the extended inlet length, L_b is the extended outlet length, k is wave number, and Y is characteristic impedance of the medium. Thus, the cancellation of troughs would occur at $m = 2n - 1$. This will result in nullification of troughs at $m = 1, 3, 5, 7, \ldots$.

Similarly, the peaks of TL of the extended outlet element occur at roots of the following equation:

$$-jY\cot(kL_b) = 0. \tag{3}$$

If the length of extended outlet $L_b = L/4$, then the resonance peaks would occur at

$$kL = 2(2n-1)\pi; \tag{4}$$

and the quarter wave resonance peaks would nullify the chamber length troughs at $m = 2, 6, 10, \ldots$.

Thus, for a double-tuned extended inlet-outlet muffler ($L_a = L/2$ and $L_b = L/4$), all troughs except those at $m = 4, 8, 12, \ldots$ are tuned out. In other words, three-fourths of the troughs are nullified, and the desirable broadband noise attenuation can be attained.[23,25] The trick, however, lies in correcting the extension lengths L_a and L_b for the evanescent modes by means of appropriate end corrections,[26] as the acoustical length of the inlet/outlet would be slightly larger than the corresponding geometrical lengths due to the presence of the evanescent higher-order modes at the junctions.[25,27]

In order to design a double-tuned extended muffler, we need to know the precise end corrections such that the chamber-length troughs are exactly cancelled by the quarter wave resonance peaks of the extended lengths. The resonance frequencies in a simple 1-D analysis are given by $-jY\cot(kL_{eff}) = 0$, where the effective length $L_{eff} = L_g + \delta$. Thus, the first resonance peak is given by

$$f_r = c_0/4(L_g + \delta). \tag{5}$$

Therefore,

$$\delta = c_0/(4f_r) - L_g; \tag{6}$$

where f_r is the first resonance frequency evaluated by means of 3-D analysis or observed in an experimental measurement,

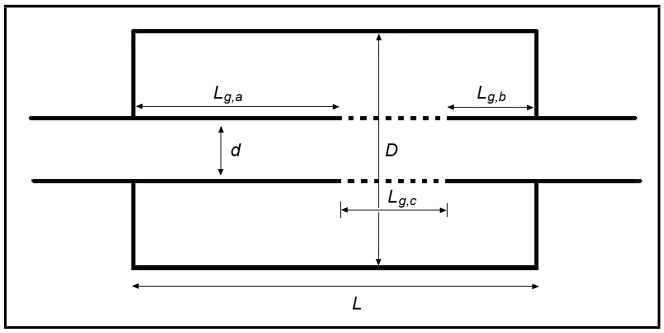

Figure 3. An extended concentric tube resonator (ECTR) used for testing.[29] ($L_{g,a} = 183$ mm, $L_{g,b} = 82.5$ mm, $L = 401$ mm, $d = 50$ mm, $D/d = 3$, $t_w = 2$ mm, $d_h = 3$ mm).

L_g is the geometrical or physical length of the extended duct, c_0 is velocity of sound at the ambient temperature, and δ is the end correction that must be added to the geometrical length. The end corrections calculated from the experimental or 3-D FEA analysis are then used in the above equations so that the effective extended lengths are calculated for ensuring the cancellation of troughs.

A change in wall thickness in the 1-D model would result in a negligible change in the cross-sectional areas of the annular cavity and, hence, the area ratio. This would not result in lateral shifting of the peaks of the quarter wave resonators. Incidentally, the 2-D or 3-D mode-matching models do not take into account the finite (non-zero) wall thickness. The 3-D FE analysis automatically takes into account the effect of wall thickness on the evanescent modes at the discontinuities and, thence, the lumped inertance and end corrections derived therefrom.

The TL measurements were performed by means of the two source-location method[28] in order to validate the 3-D FEM predictions.[27]

Predictions of the 1-D model match those of the 3-D model only when we add the end corrections to the geometric lengths for use in the 1-D model, as shown in Fig. 2. It shows that the first three peaks of the 1-D curve exactly match with those of the 3-D FEM analysis, which means the end corrections are sufficiently accurate.

TL of the corresponding expansion chamber ($L_{g,a} = L_{g,b} = 0$) is also shown in Fig. 2 in order to highlight the double-tuning effect on TL. It may be noted that the first three troughs (in fact, three-fourths of all troughs within the cut-off frequency) of the simple-chamber TL curve are raised substantially in the double-tuned chamber's TL curve. In fact, there is considerable overall lifting of the TL curve, making the double-tuned expansion chambers an important design option.

With the theoretically estimated end corrections having been validated against the 3-D FEM predictions as well as experimental results for stationary medium, the procedure was used to estimate the end corrections for different configurations. Accordingly, a parametric study was completed by means of a 3-D FEA model incorporating the wall thickness shown in Fig. 1.

A bivariate least-square analysis was conducted to evolve an approximate formula for the end correction normalized with

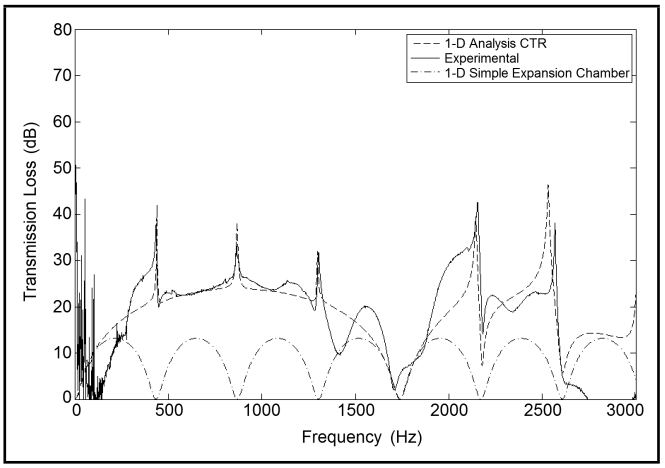

Figure 4. Comparison between 1-D prediction and experimental measurements for ECTR of Fig. 3 with 19.6% porosity.[29] ($L_{g,a} = 183$ mm, $L_{g,b} = 82.5$ mm, $L = 401$ mm, $t = 28.8\,^\circ$C).

diameter (d):

$$\frac{\delta_a}{d} = a_0 + a_1\left(\frac{D}{d}\right) + a_2\left(\frac{t_w}{d}\right) + a_3\left(\frac{D}{d}\right)^2 + a_4\left(\frac{D}{d}\frac{t_w}{d}\right) + a_5\left(\frac{t_w}{d}\right)^2; \qquad (7)$$

where $a_0 = 0.005177$, $a_1 = 0.0909$, $a_2 = 0.537$, $a_3 = -0.008594$, $a_4 = 0.02616$, $a_5 = -5.425$, and t_w is the wall thickness. In the process, it was shown that

(1) The end correction for a given extended length is the same whether it is used for extended inlet or for extended outlet.

(2) The effect of length on end corrections is marginal for $D/d \leq 3$. However, for higher diametral ratios, the effect of length is considerable.

(3) The thickness of the inlet/outlet duct wall, however, must not be neglected; it has significant influence on the end corrections, as is obvious from Eq. (7).

3. TUNING OF THE EXTENDED CONCENTRIC TUBE RESONATORS

Provision of a perforated bridge between the inlet and outlet of an extended-tube expansion chamber has the advantages of little aerodynamic noise, minimal pressure drop, and increased mechanical strength and durability. However, acoustical action of the resultant extended concentric tube resonator (ECTR) is very different from the corresponding double-tuned extended-tube chamber. Distributed-hole inertance of the CTR replaces the lumped inertance at the area discontinuities due to evanescent waves in the case of the corresponding extended-tube chambers.

A generalized procedure is given here in order to tune the concentric tube resonators. First, the effective acoustical lengths are calculated precisely by 1-D analysis of the ECTR. The difference of these acoustical lengths and the quarter wave resonance lengths (i.e., half and quarter of chamber lengths) are termed as differential lengths. Many variables, along with temperature dependence, affect the geometrical length required to tune the ECTR, so we need to use 1-D

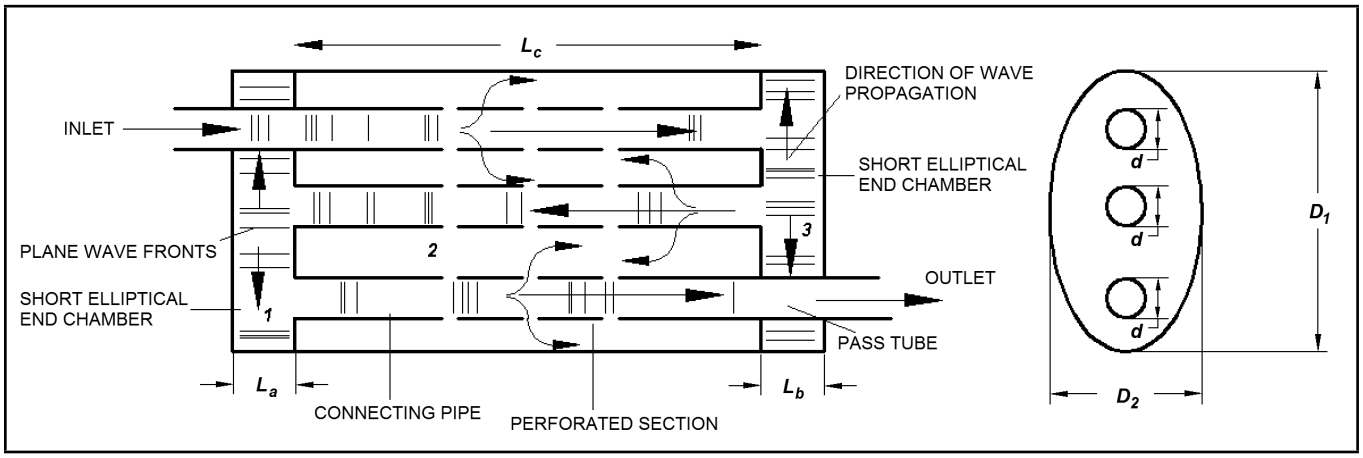

Figure 5. Double reversal end chamber muffler system.[30]

analysis to estimate the acoustical length and calculate the required physical lengths from the differential lengths and end corrections.

The differences between the two lengths (acoustical and geometric) are referred to here as end corrections. These are a consequence of the inertance of perforates.

The following least-squares fit has been developed for the differential length normalized with respect to the inner-tube diameter:[29]

$$\frac{\Delta}{d} = 4.522\sigma^2 - 2.699\sigma + 0.6643; \quad \Delta = \Delta_a = \Delta_b; \quad (8)$$

where σ is porosity of the perforates (as a fraction). Equation (8) is applicable for σ ranging from 0.1 to 0.27.

It is shown that an increase of the wall thickness by 0.5 mm or hole diameter by 1 mm increases the differential lengths by 1 mm approximately. Differential lengths are calculated from Eq. (8) above for particular porosity and inner-tube diameter, and these are used to estimate the initial values of acoustical lengths ($L_a = L/2 - \Delta$, $L_b = L/4 - \Delta$). With the help of 1-D analysis, we can increase/decrease these lengths such that the chamber length troughs are nullified effectively. The end corrections vary by –1.5 mm to +1.5 mm, and thus the required geometric lengths are estimated ($L_{g,a} = L_a - \delta_a$, $L_{g,b} = L_b - \delta_b$).

Predictions of the 1-D model match with those observed experimentally, and the end correction for this particular case is almost zero, as shown in Fig. 4. In particular, the first three peaks of the 1-D curve match exactly with experimental results.

Thus, we can make use of the 1-D analysis along with precise differential lengths and end corrections to tune the extended concentric tube resonators so as to lift or tune out three-fourths of all troughs that characterize the TL curve of the corresponding simple expansion chamber muffler. This makes the tuned ECTR a viable design option.

4. TRANSVERSE PLANE-WAVE ANALYSIS OF END CHAMBERS

Elliptical end chambers form the basis of modern-day silencing systems in automobiles. In fact, one of the present day automotive silencing systems would consist of two such end chambers connected by a uniform pipe, making use of double-flow reversal and inducing maximum impedance mismatch and thereby ensuring compactness of the design. Such a system is shown in Fig. 5, wherein the end chambers (numbered 1 and 3) and connecting pipes which also act as pass tubes are clearly shown. The lengths L_c of the connecting pipes are much greater than the lengths of the elliptical end chambers L_a.

Rather than the time-consuming FEM process, which involves geometry creation, fine meshing (requiring a lot of computer memory, especially at higher frequencies), and solving linear systems with matrix inversion routines, a simple 1-D model has been developed.

This 1-D transverse plane-wave approach can be used to obtain a transfer matrix, which is needed to cascade the matrix with the preceding and succeeding elements constituting a complex muffler. The direction of the transverse plane wave is taken along the major axis of the ellipse with the cavities above the inlet and beneath the outlet modelled as variable area resonators. The impedance of such a resonator is found using a semi-numeric technique called the matrizant approach.[30] The path between the inlet and outlet ports is modelled as a 1-D variable area duct, and the matrizant method is applied to relate the state variables at the downstream and upstream points. This rather novel method is ideally suited to incorporate the dissipative effect of mean flow at the junctions (sudden area discontinuities) of the end chamber.

Recently, this semi-analytical method has been replaced with an analytical method. The Frobenius solution of the differential equation governing the transverse plane-wave propagation is obtained.[31] By taking a sufficient number of terms of the infinite series, an approximate analytical solution so obtained shows good convergence up to about 1300 Hz and also covers most of the range of muffler dimensions used in practice. The TL performance of the muffler configurations computed by this analytical approach agrees excellently with that computed by the matrizant approach,[30] thereby offering a faster and more elegant alternate method to analyse short elliptical muffler configurations.

The perturbed continuity and momentum equations for a duct of a gradually varying cross-sectional area ($S(x)$, along the axis of plane-wave propagation) with the isentropic condition and assumption of time harmonic nature of the acoustical

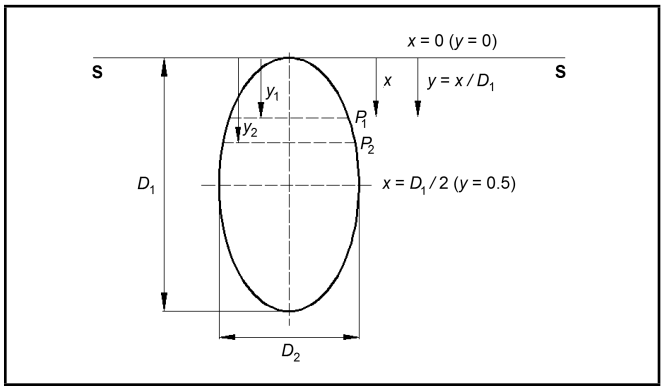

Figure 6. An elliptical cross-section having a major diameter as D_1 and minor diameter as D_2. The distance x and non-dimensional length y is measured from the top section S-S.[31]

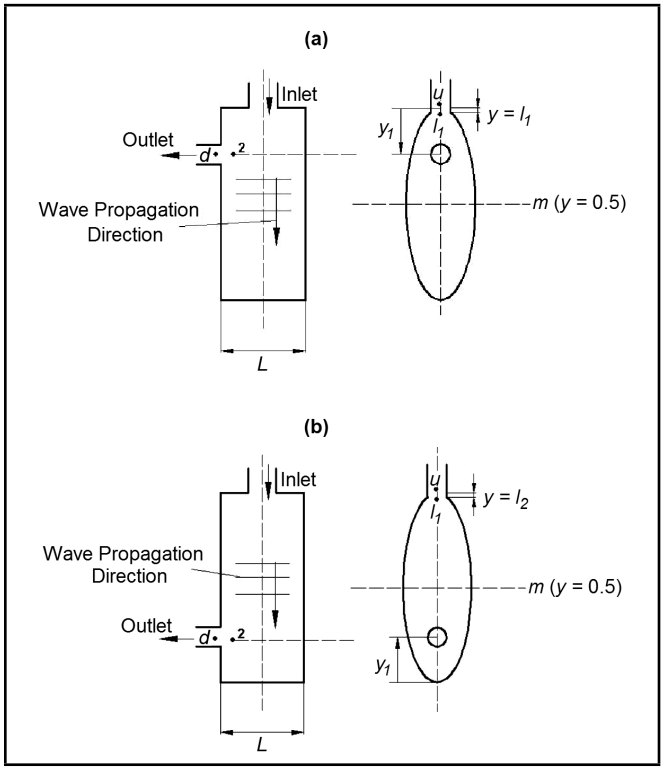

Figure 7. A short elliptical chamber with a side inlet and (a) an end outlet port on the same half as the side inlet port and (b) an end outlet port on the opposite half of the side port.[31]

pressure field yield the following 1-D equation for acoustical wave propagation:[14]

$$\frac{d^2p}{dx^2} + 1/S(x)(dS(x)/dx)\frac{dp}{dx} + k_0^2 p = 0. \tag{9}$$

The assumption of a stationary medium (i.e., the mean flow Mach number, $M = 0$) with no viscous losses is inherent in the derivation of Eq. (9). The cross-sectional area $S(x)$ for propagation along the transverse direction in a short elliptical chamber is given as[31]

$$S(x) = (2D_2L/D_1)\left(\sqrt{D_1x - x^2}\right);$$
$$\Downarrow$$
$$S(y) = (2D_2L)\left(\sqrt{y - y^2}\right); \quad y = x/D_1. \tag{10}$$

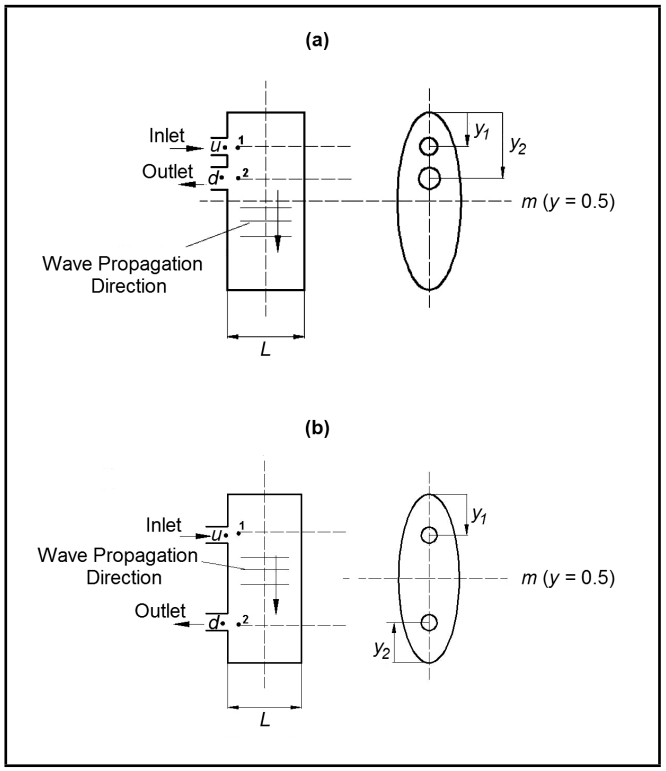

Figure 8. A short elliptical chamber with an end inlet and end outlet port with both the ports located (a) on the same half and (b) on the opposite halves.[31]

In Eq. (10), D_2 is the minor axis of the elliptical section, and L is the axial length of the chamber. The coordinate x is being measured from the top of the elliptical chamber as depicted in Fig. 6, while y is the non-dimensional counterpart of x. The region of interest where we look for a solution of Eq. (9) is $0 \leq x \leq D_1$, and in a non-dimensional form, we get $0 \leq y \leq 1$. By making use of Eq. (10), we get a non-dimensional form of Eq. (9) as

$$\frac{d^2p}{dy^2} + \left((1/2 - y)/(y - y^2)\right)\frac{dp}{dy} + \beta^2 p = 0; \quad \beta = k_0 D_1. \tag{11}$$

It is interesting to note that by replacing y with $1 - z$, such that $(0 \leq z \leq 1)$ in Eq. (11), the differential equation so obtained has the same form as Eq. (11), as shown below:

$$\frac{d^2p}{dz^2} + \left((1/2 - z)/(z - z^2)\right)\frac{dp}{dz} + \beta^2 p = 0; \quad \beta = k_0 D_1. \tag{12}$$

Hence, Eqs. (11) and (12) reveal the symmetry of the solution about $y = 0.5$ or equivalently about $x = D_1/2$. Thus, we must solve Eq. (11) for the region $0 \leq y \leq 1/2$ only, as the solution for the other half (i.e., Eq. (12) is the same as that obtained by solving Eq. (11)). In fact, we exploit this symmetry property of the differential equation governing the transverse wave propagation in elliptic ducts to find the Frobenius solution of Eq. (11), computing only as many terms as would give us a satisfactory convergence up to $y \leq 0.5$. It is important to take note of the singular points of Eq. (11) before attempting the series solution. Some typical muffler configurations of short elliptical end chambers are shown in Figs. 7 and 8. Validation of the transverse plane wave approach using Frobenius solution is provided in Fig. 9.

It is indeed observed that this analytical approach[31] is much

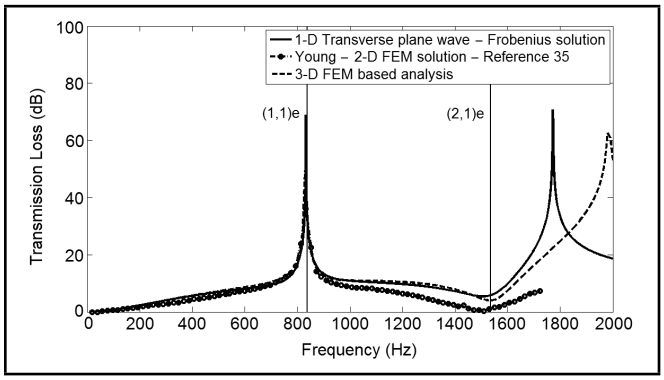

Figure 9. Validation of the transverse plane wave approach using the Frobenius solution with FEM results for the configuration of Fig. 8(a); ($y_2 = 0.5$, EOI-ECO) $D_1 = 0.24765$ m, $D_2 = 0.1016$ m, $L = 0.0508$ m, $d_1 = d_2 = 0.0508$ m, $x_1 = 0.060325$ m ($y_1 = 0.24358$).[31]

faster than the matrizant approach[30] as the present method obtains its solution in the form of a truncated polynomial series, which is very quick to evaluate. In fact, this method is particularly suited for the analysis of a short elliptical chamber with more than two ports (i.e., for a multi-port system).

The following conclusions can be made, although not all results are shown here for the sake of brevity:

(1) The short elliptical expansion chamber as well as the reversal chamber mufflers with end inlet and outlet ports (centred or offset on the major axis) shown in Fig. 8 shows dominant transverse plane wave propagation along the major axis.

(2) The acoustical attenuation characteristics of an end-offset inlet (major axis) and end-offset outlet (major axis) concentric configuration (see Fig. 8) can be modelled by considering a transverse plane wave along the major axis. For the same configuration with the circular cross-section, transverse plane wave propagation is considered by taking unequal cavities.

(3) The proposed transverse plane wave approach[30,31] enables us to incorporate the stagnation pressure losses, while 3-D approaches do not.

(4) The resultant transfer matrices may be cascaded with those of other elements, constituting a complex muffler (like the one shown in Fig. 5) in a generalized transfer-matrix based muffler software.

5. SOURCE CHARACTERIZATION OF THE ENGINE

Mufflers are generally analysed in the frequency domain using the TMM.[14] As per Thevenin's theorem, analogous to an electrical filter, the acoustical filter or muffler requires prior knowledge of the load-independent source characteristics p_s and Z_s, corresponding to the open-circuit voltage and internal impedance of an electrical source. But, the existence of unique source characteristics is practically not achievable for the engine exhaust source.[32] Moreover, because of the variable cylinder volume due to large piston motion, and the time-variant valve or port openings, we can achieve only limited success in measuring internal impedance of the exhaust/intake source.

An alternative approach is the time-domain approach in which nonlinear fluid dynamic equations are solved by means of the method of characteristics[32–34] or the 3-D finite volume method.[35] This method has the advantage of being self-sufficient inasmuch as it does not require prior knowledge of the source characteristics. However, it is much more cumbersome and time-consuming. Besides, complex muffler configurations cannot be analysed easily with the time-domain approach because of the uncertainty of boundary conditions for the multiply-connected muffler elements.

The third alternative is the hybrid approach in which we combine the time-domain analysis of the exhaust/intake source with the frequency domain analysis of the muffler downstream. Sathyanarayana and Munjal proposed a simple hybrid approach making use of an interrelationship between progressive wave variables of the linear acoustical theory and Riemann variables of the method of characteristics.[33] This approach serves well for the free radiation condition but fails in the case of complex mufflers. This limitation was removed by Hota and Munjal,[34] while retaining the associated simplicity of Sathyanarayana and Munjal's approach. Hota and Munjal incorporated the reflection of the forward wave at the exhaust valve at each of the harmonics. With this approach, they were able to predict SPL for any complex commercial muffler downstream for a single cylinder engine. However, this approach proved to be inadequate at predicting the SPL of a multi-cylinder engine, particularly for the case of a turbocharged engine.

Prasad and Crocker, based on their direct measurements of source impedance of a multi-cylinder inline compression-ignition (CI) engine,[36] proposed the anechoic source approximation: $Z_s = Y_0$. Callow and Peat also developed a relatively more realistic expression:[37]

$$Z_s(\text{exhaust}) = Y_0(0.707 - j0.707); \tag{13}$$

where Y_0 is the characteristic impedance of the exhaust pipe, $\rho_0 c_0/S$. Here, S is the area of the cross-section of the exhaust pipe, and ρ_0 and c_0 are the density and speed of sound in the exhaust gases, respectively.

Fairbrother et al. tried to extract the linear source characteristics data from nonlinear finite-volume computational fluid dynamics (CFD) simulation,[38,39] using the two-load method.[14] Knutsson and Boden then attempted to extract the intake source data from 1-D CFD simulation using the commercial software Ricardo-WAVE, which uses the finite-volume approach to solve the 1-D compressible gas dynamics equations for mass, energy and momentum.[40] The results were corroborated with the measured values quite satisfactorily. Hota and Munjal extended the work of Fairbrother et al.[38,39] to formulate the source characteristics of a CI engine as functions of the engine's physical and thermodynamic parameters and incorporated them as empirical formulas into the scheme to predict the unmuffled noise using a multi-load method.[41] Again, inspired by the work of Knutsson and Boden,[40] the investigation by Hota and Munjal[41] was extended to the intake source characterization of CI engines by Hota and Munjal.[42]

Finally, Munjal and Hota offer empirical expressions for the

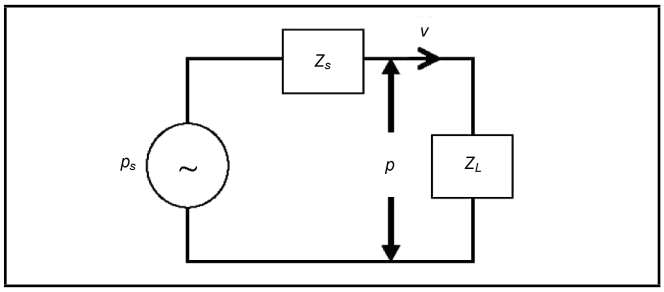

Figure 10. Electrical analogous circuit for an unmuffled system.[42]

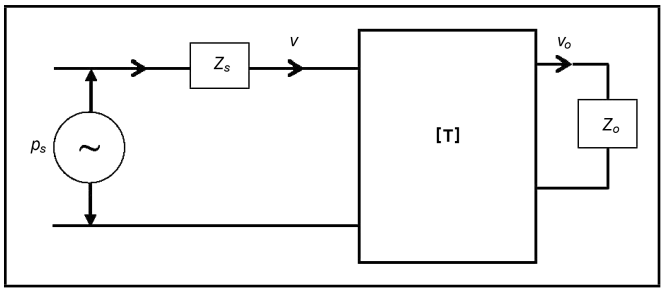

Figure 11. Electrical analogous circuit for a muffled system.[42] $[\mathbf{T}]$ is the transfer matrix of the system (filter/muffler).

source strength level (SSL) in decibels of SI engines for the intake as well as the exhaust system.[43]

A prerequisite for this investigation is to have realistic values of the pressure-time history. These were computed using the commercial software AVL-BOOST[44] for different acoustical loads. This finite-volume CFD model is used in conjunction with the two-load method to evaluate the source characteristics at a point in the exhaust pipe just downstream of the exhaust manifold. The resultant source characteristics are used with the transfer matrix-based muffler program[45] to predict the exhaust SPL of a naturally aspirated four-stroke petrol or gasoline engine. Thus, the designer will be able to compute the exhaust SPL with reasonable accuracy and thereby synthesize the required muffler configuration of a spark ignition (or gasoline) engine as well as the compression ignition (or diesel) engine.

The engine exhaust or intake source can be characterized in accordance with the electrical analogy as can be seen in Figs. 10 and 11 for the unmuffled and muffled system, respectively. Here, acoustical pressure p and volume velocity v are analogous to voltage (or electromotive force) and current in the electrical network theory, respectively.

As per the electrical analogous circuits of the unmuffled system depicted in Fig. 10, for two different acoustical loads (impedances) Z_{L1} and Z_{L2}, we can write[38]

$$p_s Z_{L1} - p_1 Z_s = p_1 Z_{L1}; \tag{14}$$

and

$$p_s Z_{L2} - p_2 Z_s = p_2 Z_{L2}. \tag{15}$$

These two equations may be solved simultaneously to obtain

$$p_s = p_1 p_2 \frac{Z_{L1} - Z_{L2}}{p_2 Z_{L1} - p_1 Z_{L2}}; \tag{16}$$

and

$$Z_s = Z_{L1} Z_{L2} \frac{p_1 - p_2}{p_2 Z_{L1} - p_1 Z_{L2}}. \tag{17}$$

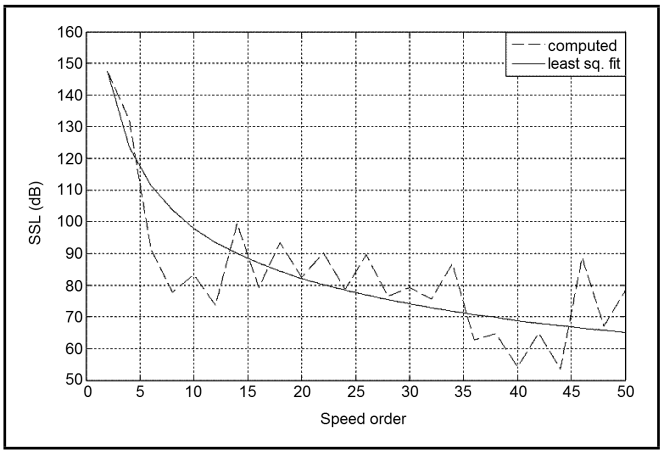

Figure 12. Values of the intake SSL as a function of speed order for a turbocharged engine.[42]

It has been observed by Hota and Munjal for the CI engines that, if a least-square fit is done on the SSL spectrum at different frequencies or speed orders, the curve goes down more or less exponentially.[41,42] Hence, the generalized formula for the SSL can be defined as

$$\text{SSL} = A \times \left(\frac{\text{speed order}}{N_{cyl}/2} \right)^B dB, \tag{18}$$

where N_{cyl} is the number of cylinders in the four-stroke cycle engine. The variable $N_{cyl}/2$ represents the speed order of the firing frequency of a four-stroke cycle engine, and constant A represents SSL at the firing frequency.

Speed order, n, of frequency f_n is defined as

$$n = \frac{f_n}{RPM/60}. \tag{19}$$

The firing frequency of a multi-cylinder engine is given by

$$\text{firing frequency} = \frac{RPM}{60} \times \frac{2}{N_{st}} \times N_{cyl}. \tag{20}$$

As there is one firing in two revolutions of a four-stroke ($N_{st} = 4$) cycle engine, the speed order of the firing frequency of a four-stroke cycle engine becomes $N_{cyl}/2$.

This kind of least-square fit has been completed to discount sharp peaks and troughs because computations have been made by assuming that speed of the engine remains absolutely constant. But, in reality, there may be around one to five percent variation in speed because the pressure-crank angle diagrams of successive cycles would never be identical.

An acoustical parametric study has been conducted for the following parameters, varying one at a time keeping other parameters constant at their default (underlined) values:

- **Turbocharged diesel engines without a catalytic converter:**
  Air fuel ratio, AFR = 18.0, **23.7**, 29.2, 38.0
  Engine speed in RPM = 1000, 1300, 1600, 2100, 2400, 3000, 3500, **4000**, 4500
  Engine capacity (displacement), V (in litres) = 1.0, 1.5, 2.0, **2.5**, 3.0, 4.0
  Number of cylinders, N_{cyl} = 1, 2, 3, **4**, 6
  So the default turbocharged engine is 4 cylinders, 2.5 litres, running at 4000 RPM, with the air-fuel ratio 23.7.

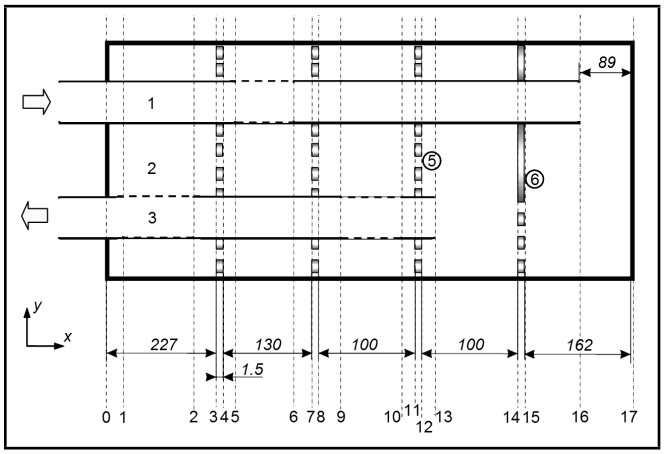

Figure 13. Schematic of a muffler with perforated elements, cross baffles, and area discontinuities (adopted from Elnady, Abom, and Allam[52]).

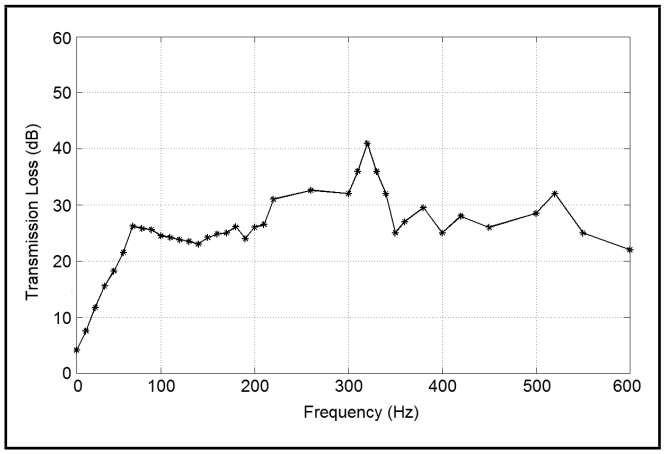

Figure 14. Measured performance of the muffler of Fig. 13 at $M = 0.1$ (adopted from Elnady, Abom, and Allam[52]).

- **Naturally aspirated diesel engines without a catalytic converter:**
  Air fuel ratio, AFR = 14.5, **17.0**, 29.0, 39.6
  Values of RPM, V, and N_{cyl} are the same as for the turbocharged engine above.

The values of A and B of SSL for the intake system of the turbocharged diesel engine have been found to be[42]

$$A = 214 \times (1 + 0.0018AFR)(1 - 0.08NS + 0.01NS^2)(1 - 0.0021V)(1 - 0.05N_{cyl}); \quad (21)$$

$$B = -0.318 \times (1 - 0.0033AFR)(1 - 0.039NS)(1 - 0.173V)(1 + 0.022N_{cyl}); \quad (22)$$

where $NS = RPM/1000$. Values of A and B for a naturally aspirated diesel engine have been found to be[41]

$$A = 189.6 \times (1 + 0.00075AFR)(1 - 0.1NS + 0.018NS^2)(1 - 0.001V)(1 - 0.028N_{cyl}); \quad (23)$$

$$B = -0.15 \times (1 + 0.0012AFR)(1 + 0.005NS)(1 - 0.0064V)(1 + 0.109N_{cyl}). \quad (24)$$

The least-squares fit values of A and B for the intake and exhaust systems of other types of engines are given by Hota and Munjal.[41,42]

6. MULTIPLY-CONNECTED MUFFLERS

The TMM is applicable to cascaded 1-D systems. Often, automotive mufflers make use of multiply-connected mufflers in order to reduce mean pressure drop (back pressure) as well as to satisfy logistic constraints. Analysing such like elements (see Figs. 5 and 13, for example) has the additional advantage of higher TL or IL over a wide frequency range.

Glav and Abom developed a general formalism for analysing acoustical two-port networks.[46] Panigrahi and Munjal proposed an algorithm which can be used to analyse automotive mufflers based on network theory.[47] Dowling and Peat used the transfer matrix approach to analyse silencers of any given geometry using a path fraction algorithm which reduces every sub-system to an effective two-port system using a data logging scheme.[48] Panigrahi and Munjal proposed a geometry-based volume synthesis algorithm using transfer matrices to analyse commercially used automotive mufflers.[49] Kar et al. presented a boundary-conditions transfer algorithm[50] for analysing multiple-duct variable area perforated tube resonators.[51] Recently, Elnady et al.[52] proposed a new segmentation approach based on two-port analysis techniques in order to model perforated pipes using general two-port codes, which are widely available.[53] The multiply-connected perforated element mufflers can be designed to obtain high broadband IL as well as remarkably low back pressure.[52,54] In particular, the TL trough is lifted substantially, resulting in a considerable increase in the overall IL at all engine speeds, as shown in Fig. 14.

7. BREAKOUT NOISE FROM THE MUFFLER SHELL AND END PLATES

Noise generated by engines, compressors, fans, etc. is radiated out into the atmosphere at the tail pipe end of the muffler axially and also as breakout noise from the walls of the muffler shell and the end plates in the transverse direction.

In a comprehensive review article, Cummings[55] identified the main physical processes involved in acoustical breakout and break in through duct walls and speculated on the possible direction of future research. Soon thereafter, a study on sound transmission characteristics of a cylindrical shell using analytical and experimental models was presented by Lee and Kim.[56]

A fraction W_r of the total incident power, W_i, into a muffler is reflected back to the source at the inlet; a fraction W_{diss} is dissipated; a portion W_{rad} is radiated from the shell and the end plates; and the remaining power, W_{to}, is transmitted through the outlet. Figure 15 shows a schematic of these components on the muffler.

The overall or net TL[57] is composed of an axial component and a transverse component and these are defined as follows:

- The axial TL, TL_a, is defined as

$$TL_a = 10 \log \left(\frac{W_i}{W_{to}} \right). \quad (25)$$

- The transverse TL, TL_{tp}, is defined as

$$TL_{tp} = 10 \log \left(\frac{W_i}{W_{rad}} \right). \quad (26)$$

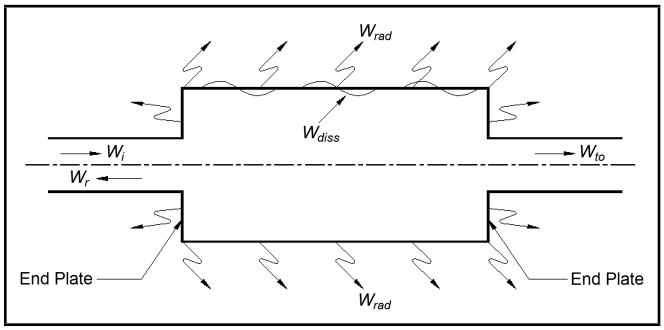

Figure 15. Schematic of the breakout noise from the muffler shell and end plates.

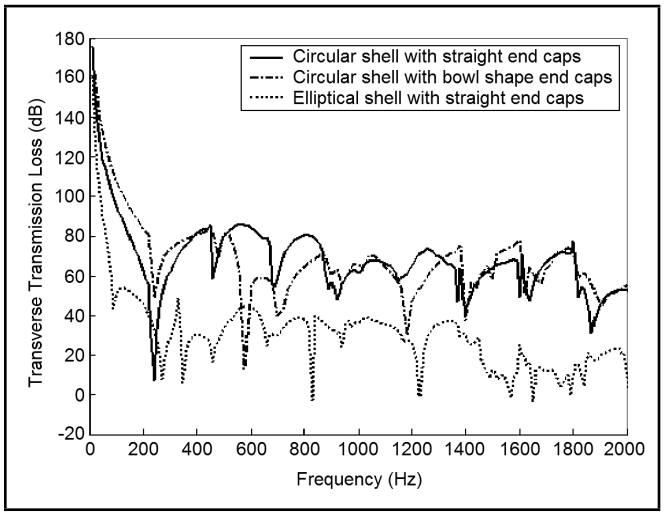

Figure 16. Computed transverse TL of an expansion chamber muffler (adopted from Narayana and Munjal[58]).

- The net TL, TL_{net}, is defined as[57]

$$TL_{net} = 10\log\left(\frac{W_i}{W_{to}+W_{rad}}\right) = -10\log\left(10^{-0.1TL_a}+10^{-0.1TL_{tp}}\right). \quad (27)$$

For proper designing of the silencer systems, the axial TL (TL_a) as well as the transverse TL (TL_{tp}) should be high enough so that the net TL (TL_{net}) is adequate.

Narayana and Munjal[58] made use of the FEM-BEM simulation of a typical circular muffler to investigate the relative importance of the muffler shell and end plates. A comparison of transverse TL of an experimental expansion chamber muffler for equivalent elliptical and bowl-type end plate mufflers is shown in Fig. 16. It can be seen that the circular shell with bowl-type end caps is the best from the breakout noise point of view, particularly at low frequencies (below 400 Hz), which are most important inasmuch as the engine exhaust noise peaks at the firing frequency and a couple of harmonics thereof.

The parametric studies based on FEM-BEM simulation led to the following design guidelines:[58]

(1) End plates are more critical than the shell of the same thickness.

(2) Circular shells are the best in this regard, although logistical constraints under a passenger car may necessitate elliptic muffler configurations.

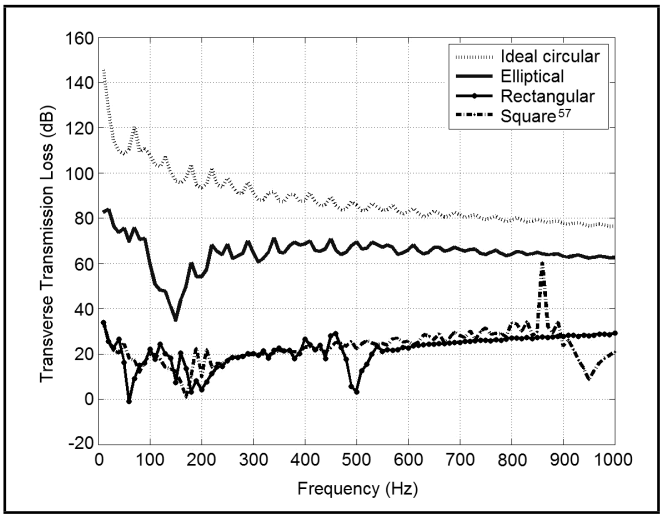

Figure 17. Comparison of the transverse TL for ideal circular duct, square duct, elliptical duct, and rectangular duct for open termination.[60]

(3) For a typical 20 cm diameter circular muffler, 2 mm thickness is adequate for the end plates (or caps) as well as the shell.

(4) Dish-type end plates are better than flat end plates as well as the hemispherical ones.

Cummings, Chang, and Astley[59] gave theoretical consideration to sound transmission through the walls of distorted circular ducts for plane wave transmission within the duct. The transmission mechanism is essentially that of mode coupling, whereby higher structural modes in the duct walls are excited because of the wall distortion by the internal sound field. Recently, Munjal et al.[60] extended this approach to predict the breakout noise from an elliptical duct of finite length. As shown in Fig. 17, deviation from circularity decreases the transverse TL and hence increases the breakout noise substantially—that is why transverse TL of rectangular (or square) ducts is the lowest,[61] which accounts for cross talk in the HVAC systems. This indicates the importance of proper design of shell and plates[58] as well as the inner acoustical elements of the muffler.

8. DIESEL PARTICULATE FILTERS AND INLET AIR CLEANERS

Currently, the most effective method practiced to reduce particulate material emission is the installation of a diesel particulate filter (DPF) in the engine exhaust zone. Similarly, intake air cleaner is used to filter out dust particles from the fresh air entering the cylinder. Both of these elements offer considerable TL or IL and therefore need to be modelled for acoustics, too.

The procedure of diesel particulate material removal includes the use of a particulate filter that allows simultaneous soot filtration and combustion. Ceramic foams are currently considered one of the best filter elements, which allow for efficient soot filtration. Apart from this, DPF is sometimes associated with chemical reactions that prevent the unrestricted motion of the harmful gases generated during combustion to atmosphere and convert them to some non-toxic gases before they are emitted to atmosphere.

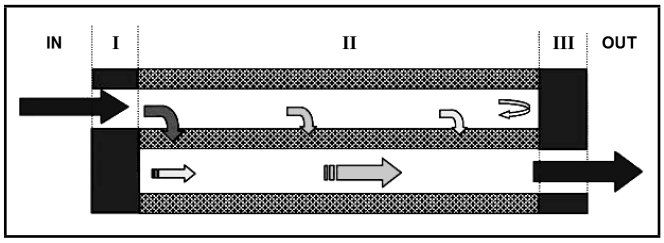

Figure 18. Five sections in a unit cell of DPF.[63,64]

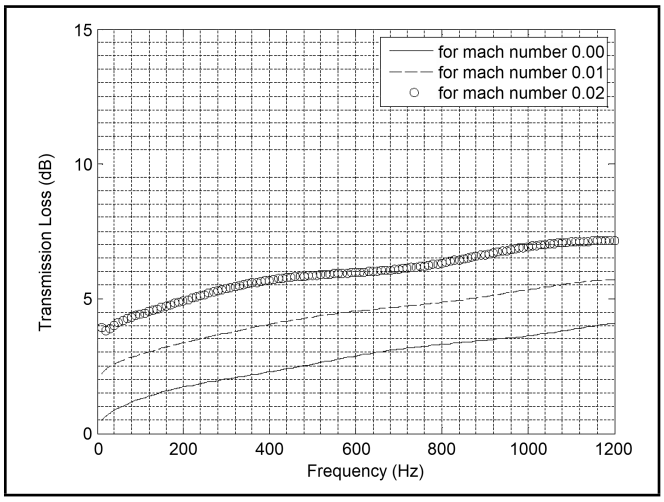

Figure 19. Effect of Mach number on TL of a typical DPF.[64]

A typical diesel particulate figure (DPF) consists of a large number of parallel narrow channels with alternate closed ends. A typical unit cell or pair of these channels is shown in Fig. 18.

Dokumaci derived an approximate dispersion equation for sound waves in a narrow pipe with ambient pressure and temperature gradients.[62] The effect of this variation on real and imaginary parts of a propagation constant was found to be trivial and therefore can be neglected for all practical purposes in order to simplify the problem. Allam and Abom performed mathematical analysis as well as experimentation on diesel particulate filters.[63] Based on Dokumaci's work,[62] Allam and Abom modelled sound propagation in an array of narrow porous channels with application to diesel particulate filters.[64] In Allam and Abom's work, the viscous and thermal losses along the narrow channels are duly considered. The solution of the convective acoustical wave equation helped to compute the transfer matrix of the two ports, which eventually is required to calculate TL. In addition to this, a revised solution for the 1-D wave model, including the effect of Kirchhoff's solution for cylindrical pipes, is discussed. The results show that both the numerical as well as the modified 1-D model produce TL values that tally with experimental results up to frequencies of 1200 Hz.

The formulation starts with the two basic equations of acoustics and fluid mechanics:[64]

(1) The equation of continuity:

$$\frac{\partial \rho_j}{\partial t} + U_{0j}\frac{\partial \rho_j}{\partial x} + \rho_{0j}\frac{\partial u_j}{\partial x} = (-1)^j \frac{4\rho_w}{d_{hj}} u_w; \qquad (28)$$

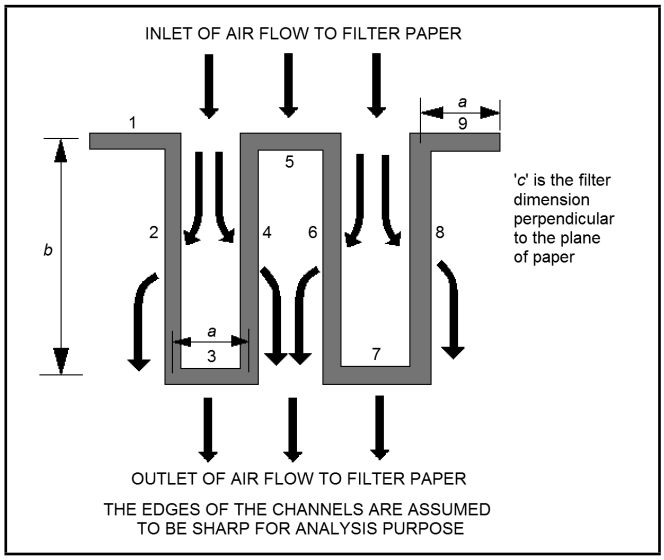

Figure 20. Flow of air through filter paper.[66]

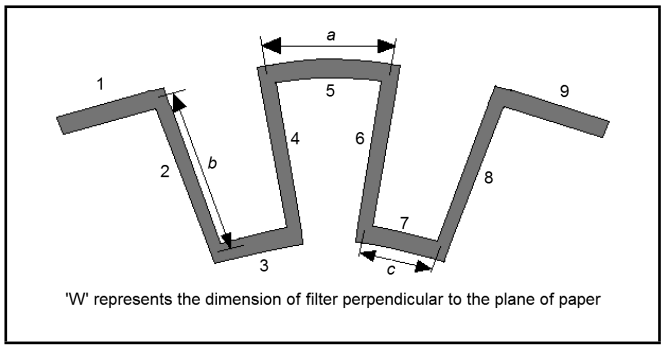

Figure 21. Schematic representation of part of circular filter element.[66]

(2) The equation of momentum:

$$\rho_{0j}\left(\frac{\partial}{\partial t} + U_{0j}\frac{\partial}{\partial x}\right) u_j = -\frac{\partial p_j}{\partial x} - \alpha_j u_j. \qquad (29)$$

Here $j = 1, 2$ denote the inflow channel (1) and outflow channel (2), respectively; u_w = particle velocity through the wall; ρ_w = gas density in the porous wall; d_h = width of the quadratic channels; and α = channel pressure drop factor.

It is possible to improve the desired results by assuming thermo-viscous wave field with characteristics defined by Kirchhoff's solution for a cylindrical pipe. The basis of this model is to drop the viscous friction factor α_j and substitute the following values of speed of sound (c_j) and density (ρ_{0j}):[65]

$$\rho_j = \rho_{0j}/(1 - F(s_j));$$
$$c_j = c_{0j}^{ad}(1 - F(s_j))^{1/2}/[1 + (\gamma - 1)F(\xi_j s_j)]^{1/2}. \qquad (30)$$

Here, c_{0j}^{ad} is the adiabatic speed of sound in channel number j, and

$$F(s) = (2/s\sqrt{-i})(J_1(s\sqrt{-i})/J_0(s\sqrt{-i})); \qquad (31)$$

where J is the Bessel function of first kind, s = shear wave number $= \sqrt{\rho_{0j}\omega/\mu_j}$, ξ = Prandtl number $= \sqrt{\mu_j C_{pj}/k_{thj}}$, μ = dynamic viscosity, C_p = specific heat at constant pressure, and k_{th} = thermal conductivity.

The porous walls of the DPF are very thin. So, the steady-state flow resistance will apply also to the acoustical fields. A

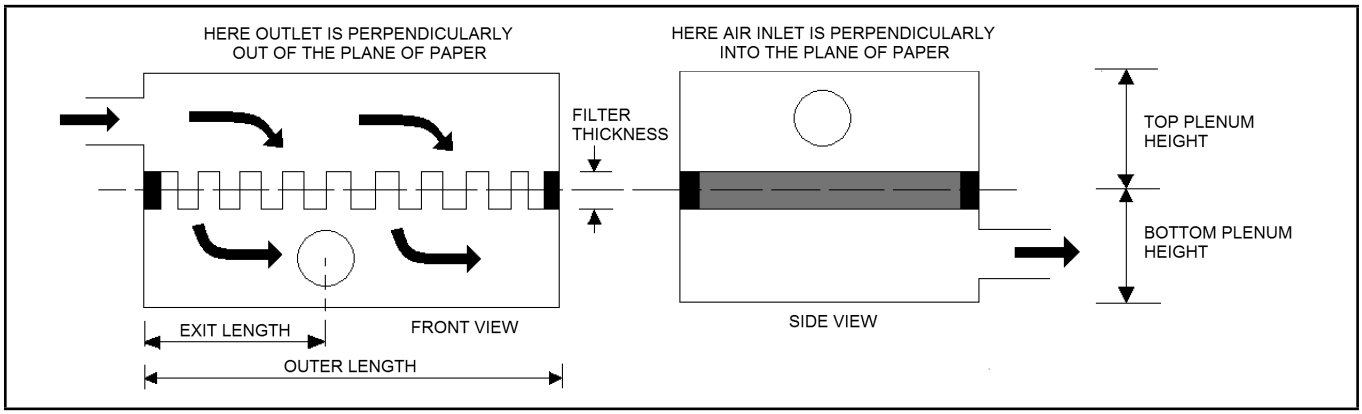

Figure 22. Schematic representation of a RAITO cleaner.[66]

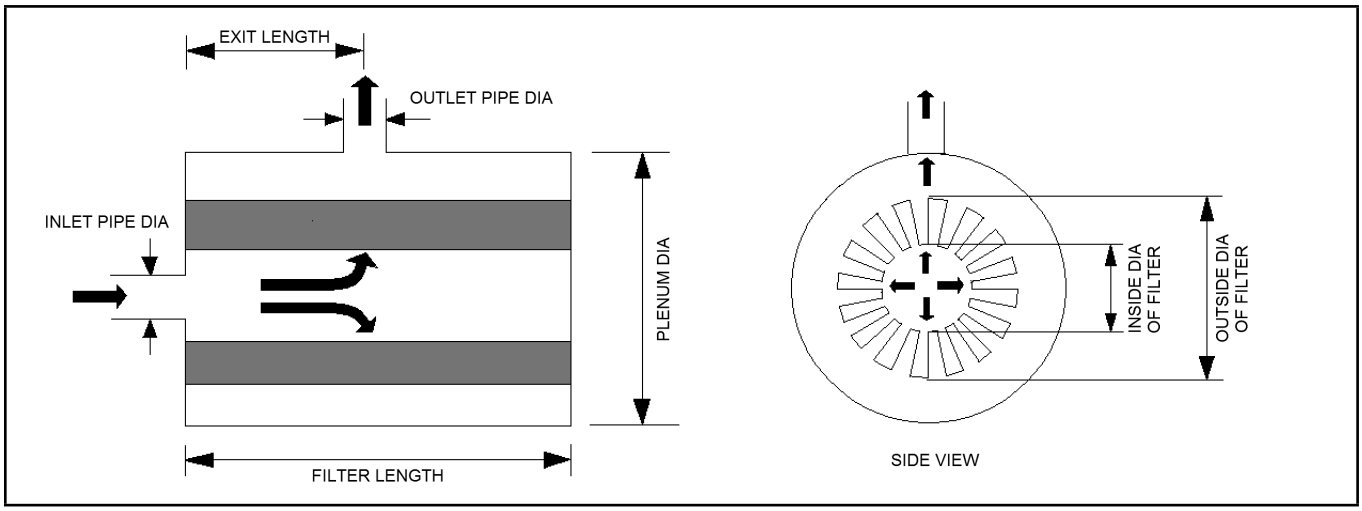

Figure 23. Schematic representation of different views of circular CAITO air cleaner.[66]

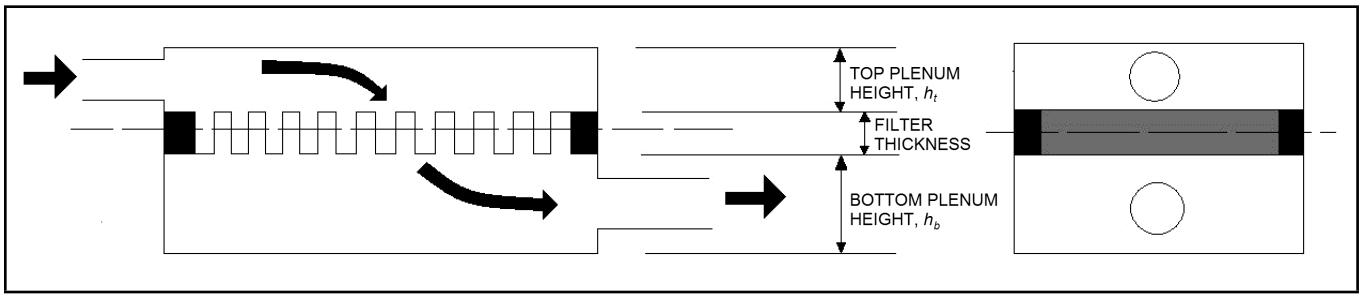

Figure 24. Schematic representation of an RAIAO air cleaner.[67]

frequency-independent wall resistance will then be

$$R_w = (p_1 - p_2)/u_w. \tag{32}$$

In terms of porous wall properties, the wall resistance can be given as[64]

$$R_w = \mu_w h_t/\sigma_w; \tag{33}$$

where $\mu_w =$ dynamic viscosity of the fluid passing through the filter wall, $h_t =$ filter wall thickness, and $\sigma_w =$ permeability of the wall. Further analysis proceeds as for the interacting perforated ducts.[15,64] Figure 19 indicates that increased flow velocity would ensure better acoustical performance of the DPF.

A generically similar application is the air cleaners used in the intake systems of the internal combustion engines for reducing mechanical wear inside the engine. Though there are several configurations of cleaner boxes available in the automobile market, recently Munjal and Mukherjee have presented a 1-D or plane wave analysis of the following:

(a) rectangular axial-inlet transverse-outlet (RAITO) air cleaners shown in Figs. 22 and 20,[66]

(b) circular axial-inlet transverse-outlet (CAITO) air cleaners shown in Figs. 23 and 21,[66]

(c) rectangular axial-inlet axial-outlet (RAIAO) air cleaners shown in Fig. 24,[67]

(d) rectangular transverse-inlet transverse-outlet (RTITO) air

cleaners shown in Fig. 25.[67]

The 1-D acoustical analysis model proposed by Munjal and Mukherjee[66,67] makes use of an analogy to a two-duct perforated cross flow element.[7] Results of the 1-D analysis were validated with those of the 3-D finite element software SYSNOISE.

In the RAITO filter cleaner shown in Fig. 22, the mean flow enters axially in the top plenum, passes through the filter element, and then exits the bottom plenum in the transverse direction. Typical thickness of the filtering element is around 25 mm, and the paper that the filter is made of has a thickness of around 0.35–1 mm. The filter paper is treated as a uniformly perforated element. However, since the filter configuration cannot be treated as a uniformly perforated element in a single plane, we need to modify the resistance value of the total filter accordingly. This can be done as follows.

It is obvious from Fig. 20 that in this configuration, the flow gets more than one path to traverse from the top plenum to the bottom plenum, compared to a configuration in which the filter paper would lie flat on a single plane without any waviness. For this reason, due to the special configuration of the filtering element, we need to modify the nominal resistance of the filter paper. To get an idea of how this modification can be done, in Fig. 20, two open and three closed channels are drawn, but the analysis is based on n pairs of such channels. The division of flow corresponds to resistances in parallel. Thus,

$$1/R_{eq} = (2n+1)/R_1 + 2n/R_2. \tag{34}$$

Now,

$$\begin{aligned} R_{eq} &= \frac{((p_1 - p_2)/u_f)_{eq}}{(2n+1)ac}; \\ R_1 &= (1/ac)(\mu h/\sigma); \\ R_2 &= (1/bc)(\mu h/\sigma); \end{aligned} \tag{35}$$

where p_1 and p_2 are acoustical pressures in the two regions across the filter element, u_f is the surface averaged particle velocity through the filter element, μ is dynamic viscosity of air, h is filter paper thickness, σ is permeability of the filter paper, and $\mu h/\sigma$ is the resistance provided by the filter wall.[68]

Substituting all these values in Eq. (34) yields

$$\zeta \equiv (p/u)_{eq} = (\mu h/\sigma)\left[a/\left\{a + 2n/(2n+1)b\right\}\right]. \tag{36}$$

In all practical cases, n is a large number (varying from 20–100). Therefore, $2n/(2n+1) \approx 1$. Thus,

$$\zeta = (\mu h/\sigma)\left[a/(a+b)\right]. \tag{37}$$

Typical results of the analysis[66,67] are shown in Figs. 26 and 27. The data assumed to generate these plots are as follows (see Fig. 22): Cleaner outer length = 275 mm; cleaner outer width = 170 mm; filter thickness = 20 mm; inside height of the top plenum = 60 mm; inside height of the bottom plenum = 60 mm; inlet pipe diameter = 40 mm; outlet pipe diameter = 40 mm; exit length = 137.5 mm; number of channel pairs = 80 (approximately); filter paper permeability = 1×10^{-12} m^2 (range of permeability is obtained from Qi and Uesaka[69]).

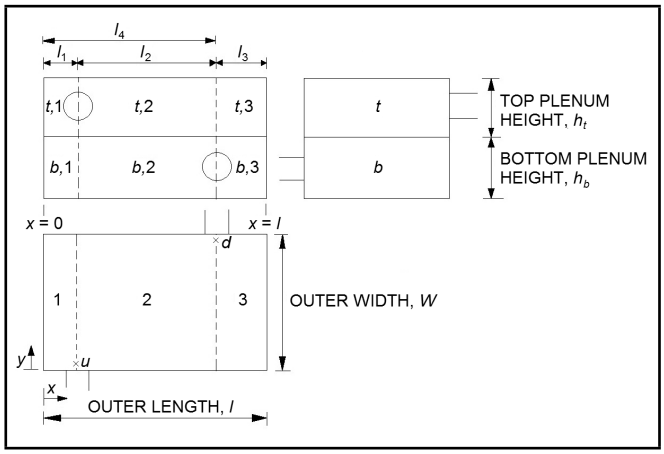

Figure 25. Schematic representation of an RTITO air cleaner.[67]

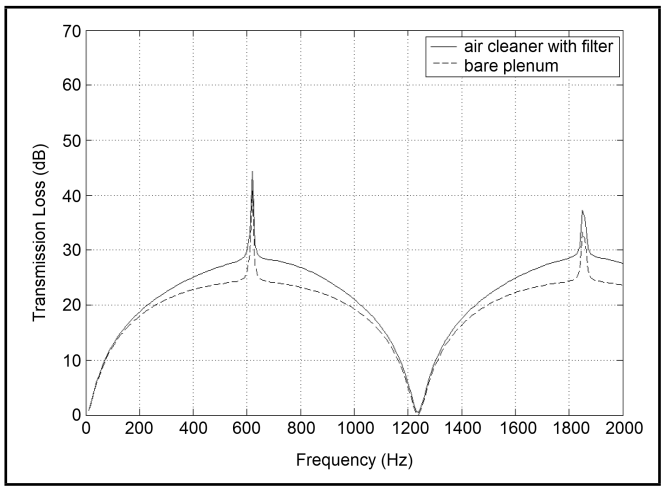

Figure 26. Comparison of complete filter box effect with that of the plenum alone.[66]

Figure 26 brings out the role of the filter paper (the difference between the two curves represents that effect). Results of the 1-D prediction model above are validated with the 3-D finite element predictions in Fig. 27, where the filter element is modeled by a transfer impedance interface condition ($(p_1 - p_2)/u_f = \mu h/\sigma$) between two neighbouring finite elements.

It should be noted that up to 700 Hz, the 1-D model and 3-D FEM results are in good agreement with each other. Beyond that frequency, two curves start deviating from each other. This is not a limitation since our main interest lies in the low-frequency zone, where the intake SPL is relatively high. One important note should be highlighted here. In Fig. 27, one resonance peak is observed at 1000 Hz due to wave propagation in the y-direction in the configuration of Fig. 22. In our 1-D model, considering wave propagation in the x-direction, we cannot capture this resonance peak in our TL versus frequency curve. This is, of course, one of the limitations of this kind of 1-D analytical formulation.

Similar inferences have been made for the RAIAO air cleaner of Fig. 24 and the RTITO air cleaner of Fig. 25.[67]

Major conclusions of this investigation are as follows:

(a) Typical inlet air cleaner acts as a simple expansion chamber. The filter element enhances its TL by means of inline

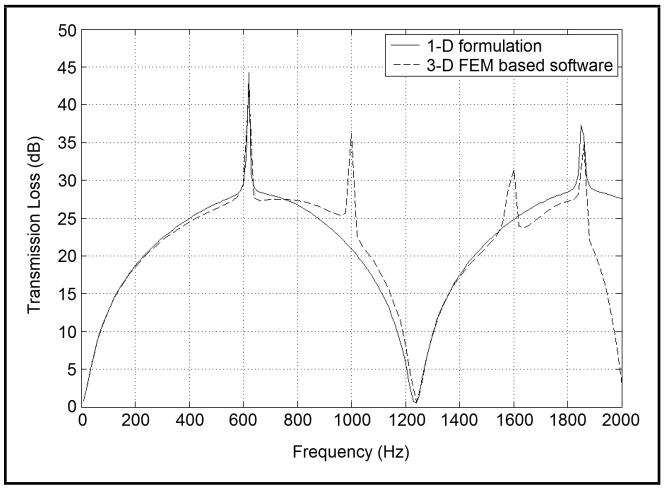

Figure 27. Validation of 1-D analysis results with the 3-D FEM-based software.[66]

aeroacoustical resistance, which is the primary element or actor in a diesel particulate filter in the exhaust system.

(b) Reduced permeability or increased filter paper or material thickness results in an increase in the overall TL of the air cleaner assembly.

(c) The 1-D analysis presented by Munjal and Mukherjee[66,67] is adequate for most practical conditions like the intake system of an IC engine in which the unmuffled intake noise is predominant at the first few harmonics of the firing frequency.

9. CONCLUSIONS

In this review paper, recent advances in the theory and design of double-tuned expansion chamber and the extended concentric tube resonators, transverse plane wave analysis of short elliptical end chambers, acoustical source characterization of the intake as well as exhaust systems of reciprocating internal combustion engines, analysis of multiply-connected element mufflers, breakout noise of non-circular muffler shells, and analysis of diesel particulate filters and inlet air cleaners have been discussed. These are some of the topics in muffler acoustics that have a direct bearing on design of efficient mufflers for the intake as well as exhaust systems of IC engines. An equally important design parameter is the mean pressure drop or back pressure, which has been mentioned incidentally at a couple of instances, although it deserves a thorough study by itself. Recently, Elnady, Elsadany, and Abom[70] have presented a two-port method for flow and pressure drop calculation as well as acoustical analysis of complex perforated-element automotive mufflers.

ACKNOWLEDGEMENTS

The author would like to thank the Department of Science and Technology of the Government of India for providing the computational and experimental facilities through the Facility for Research in Technical Acoustics since 1998.

REFERENCES

[1] Olson, H. F. *Dynamical analogies*, 2nd edition, Van Nostrand, (1958).

[2] Rayleigh, J. W. S. *The theory of sound*, 2nd edition, McMillan, London, (1894).

[3] Davis Jr., D. D., Stokes, M., Moore, D., and Stevens, L. Theoretical and experimental investigation of mufflers with comments on engine exhaust muffler design, NACA Report 1192, (1954).

[4] Fukuda, M. A study on the exhaust mufflers of internal combustion engines, *Bull. JSME*, **6** (22), (1963).

[5] Munjal, M. L., Sreenath, A. V., and Narasimhan, M. V. An algebraic algorithm for the design and analysis of linear dynamical systems, *Journal of Sound and Vibration*, **26** (2), 193–208, (1973).

[6] Munjal, M. L., Narasimhan, M. V., and Sreenath, A. V. A rational approach to the synthesis of one-dimensional acoustic filters, *Journal of Sound and Vibration*, **29** (3), 263–280, (1973).

[7] Munjal, M. L. A rational synthesis of vibration isolators, *Journal of Sound and Vibration*, **39** (2), 247–265, (1975).

[8] Morfey, C. L. Sound generation and transmission in duct with flow, *Journal of Sound and Vibration*, **14** (1), 37–55, (1971).

[9] Alfredson, R. J. and Davies, P. O. A. L. The radiation of sound from the engine exhaust, *Journal of Sound and Vibration*, **13** (4), 389–408, (1970).

[10] Munjal, M. L. Velocity ratio-cum-transfer matrix method for evaluation of a muffler with mean flow, *Journal of Sound and Vibration*, **39** (1), 105–119, (1975).

[11] Sullivan, J. W. and Crocker, M. J. Analysis of concentric tube resonators having un-partitioned cavities, *Journal of the Acoustical Society of America*, **64**, 207–215, (1978).

[12] Sullivan, J. W. A method for modelling perforated tube muffler components. I. Theory, II. Applications, *Journal of the Acoustical Society of America*, **66**, 772–788, (1979).

[13] Munjal, M. L., Narayana Rao, K., and Sahasrabudhe, A. D. Aeroacoustic analysis of perforated muffler components, *Journal of Sound and Vibration*, **114** (2), 173–188, (1987).

[14] Munjal, M. L. *Acoustics of ducts and mufflers*, Wiley-Interscience, New York, (1987).

[15] Peat, K. S. A numerical decoupling analysis of perforated pipe silencer element, *Journal of Sound and Vibration*, **123**, 199–212, (1988).

[16] Munjal, M. L., Krishnan, S., and Reddy, M. M. Flow-acoustic performance of the perforated elements with application to design, *Noise Control Engineering Journal*, **40** (1), 159–167, (1993).

[17] Gogate, G. R. and Munjal, M. L. Analytical and experimental aeroacoustic studies of open-ended three-duct perforated elements used in mufflers, *Journal of the Acoustical Society of America*, **97** (5), 2919–2927, (1995).

[18] Munjal, M. L. Plane wave analysis of side inlet/outlet chamber mufflers with mean flow, *Applied Acoustics*, **52** (2), 165–175, (1997).

[19] Munjal, M. L., Behera, B. K., and Thawani, P. T. An analytical model of the reverse flow, open end, extended perforated element muffler, *International Journal of Acoustics and Vibration*, **2** (2), 59–62, (1997).

[20] Munjal, M. L. Analysis of a flush tube three-pass perforated element muffler by means of transfer matrices, *International Journal of Acoustics and Vibration*, **2** (2), 63–68, (1997).

[21] Kar, T. and Munjal, M. L. Analysis and design of conical concentric tube resonators, *Journal of the Acoustical Society of America*, **116** (1), 74–83, (2004).

[22] Kar, T. and Munjal, M. L. Generalized analysis of a muffler with any number of interacting ducts, *Journal of Sound and Vibration*, **285** (3), 585–596, (2005).

[23] Munjal, M. L., Galaitsis, A. G., and Ver, I. L. Passive silencers, In I. L. Ver and L. L. Beranek, eds., *Noise and vibration control engineering*, John Wiley, New York, (2006).

[24] Munjal, M. L. Muffler acoustics, In F. P. Mechel, ed., *Formulas of acoustics*, Springer Verlag, Berlin, (2002).

[25] Munjal, M. L. and Gowri, S. Theory and design of tuned extended tube chambers and concentric tube resonators, *Journal of the Acoustical Society of India*, **36** (2), 53–71, (2009).

[26] Karal, F. C. The analogous impedance for discontinuities and constrictions of circular cross-section, *Journal of the Acoustical Society of America*, **25** (2), 327–334, (1953).

[27] Chaitanya, P. and Munjal, M. L. Effect of wall thickness on the end corrections of the extended inlet and outlet of a double-tuned expansion chamber, *Applied Acoustics*, **72** (1), 65–70, (2011).

[28] Munjal, M. L. and Doige, A. G. Theory of a two source-location method for direct experimental evaluation of the four-pole parameters of an aeroacoustic element, *Journal of Sound and Vibration*, **141** (2), 323–334, (1990).

[29] Chaitanya, P. and Munjal, M. L. Tuning of the extended concentric tube resonators, *SAE International Symposium on International Automotive Technology* (SIAT-2011), 2011-26-0070, ARAI, Pune, India, (2011).

[30] Mimani, A. and Munjal, M. L. Transverse plane-wave analysis of short elliptical end-chamber and expansion-chamber mufflers, *International Journal of Acoustics and Vibration*, **15** (1), 24–38, (2010).

[31] Mimani, A. and Munjal, M. L. Transverse plane wave analysis of short elliptical chamber mufflers — An analytical approach, *Journal of Sound and Vibration*, **330**, 1472–1489, (2011).

[32] Gupta, V. H. and Munjal, M. L. On numerical prediction of the acoustical source characteristics of an engine exhaust system, *Journal of the Acoustical Society of America*, **92** (5), 2716–2725, (1992).

[33] Sathyanarayana, Y. and Munjal, M. L. A hybrid approach for aero-acoustic analysis of the engine exhaust system, *Applied Acoustics*, **60**, 425–450, (2000).

[34] Hota, R. N. and Munjal, M. L. A new hybrid approach for thermo-acoustic modeling of engine exhaust system, *International Journal of Acoustics and Vibration*, **9** (3), 129–138, (2004).

[35] Young, C.-I. J. and Crocker, M. J. Prediction of transmission loss in mufflers by the finite element method, *Journal of the Acoustical Society of America*, **57** (1), 144–148, (1975).

[36] Prasad, M. G. and Crocker, M. J. On the measurement of the internal source impedance of a multi-cylinder engine exhaust system, *Journal of Sound and Vibration*, **90**, 491–508, (1983).

[37] Callow, G. D. and Peat, K. S. Insertion loss of engine inflow and exhaust silencers, I Mech. E C19/88:39-46, (1988).

[38] Fairbrother, R., Boden, H., and Glav, R. Linear acoustic exhaust system simulation using source data from linear simulation, SAE Technical Paper 2005-01-2358, (2005).

[39] Boden, H., Tonse M., and Fairbrother, R. On extraction of IC-engine acoustic source data from non-linear simulations, *Proceedings of the Eleventh International Congress on Sound and Vibration* (ICSV11), St. Petersburg, Russia, (2004).

[40] Knutsson, M. and Boden, H. IC-Engine intake source data from non-linear simulations, SAE Technical Paper 2007-01-2209, (2007).

[41] Hota, R. N. and Munjal, M. L. Approximate empirical expressions for the aeroacoustic source strength level of the exhaust system of compression ignition engines, *International Journal of Aeroacoustics*, **7** (3–4), 349–371, (2008).

[42] Hota, R. N. and Munjal, M. L. Intake source characterization of a compression ignition engine: Empirical expressions, *Noise Control Engineering Journal*, **56** (2), 92–106, (2008).

[43] Munjal, M. L. and Hota, R. N. Acoustic source characteristics of the exhaust and intake systems of a spark ignition engine, Paper No. 78, *Inter-Noise 2010*, Lisbon, Portugal, (2010).

[44] BOOST Version 5.0.2, AVL LIST GmbH, Graz, Austria, (2007).

[45] Munjal, M. L., Panigrahi, S. N., and Hota, R. N. FRITA-muff: A comprehensive platform for prediction of unmuffled and muffled exhaust noise of I.C. engines, *Proceedings of the Fourteenth International Congress on Sound and Vibration* (ICSV14), Cairns, Australia, (2007).

[46] Glav, R. and Abom, M. A generalized formalism for analyzing acoustic 2-port networks, *Journal of Sound and Vibration*, **202** (5), 739–747, (1997).

[47] Panigrahi, S. N. and Munjal, M. L. Plane wave propagation in generalized multiply connected acoustic filters, *Journal of the Acoustical Society of America*, **118** (5), 2860–2868, (2005).

[48] Dowling, J. F. and Peat, K. S. An algorithm for the efficient acoustic analysis of silencers of any general geometry, *Applied Acoustics*, **65**, 211–217, (2004).

[49] Panigrahi, S. N. and Munjal, M. L. A generalized scheme for analysis of multifarious commercially used mufflers, *Applied Acoustics*, **68**, 660–681, (2007).

[50] Kar, T. and Munjal, M. L. An inherently stable boundary-condition-transfer algorithm for muffler analysis, *Journal of the Acoustical Society of America*, **118** (1), 60–71, (2005).

[51] Kar, T., Sharma, P. P. R., and Munjal, M. L. Analysis of multiple-duct variable area perforated tube resonators, *International Journal of Acoustics and Vibration*, **11** (1), 19–26, (2006).

[52] Elnady, T., Abom, M., and Allam, S. Modeling perforates in mufflers using two-ports, *ASME Journal of Vibration and Acoustics*, **132**, 1–11, (2010).

[53] Elnady, T. and Abom, M. SIDLAB: New 1-D sound propagation simulation software for complex duct networks, *Proceedings of the Thirteenth International Congress on Sound and Vibration* (ICSV13), Vienna, (2006).

[54] Panigrahi, S. N. and Munjal, M. L. Backpressure considerations in designing of cross flow perforated-element reactive silencers, *Noise Control Engineering Journal*, **55** (6), 504–515, (2007).

[55] Cummings, A. Sound transmission through duct walls, *Journal of Sound and Vibration*, **239** (4), 731–765, (2001).

[56] Lee, J. H. and Kim, J. Study on sound transmission characteristics of a cylindrical shell using analytical and experimental models, *Applied Acoustics*, **64**, 611–632, (2003).

[57] Munjal, M. L. Prediction of the break-out noise of the cylindrical sandwich plate muffler shells, *Applied Acoustics*, **53**, 153–161, (1998).

[58] Narayana, T. S. S. and Munjal, M. L. Computational prediction and measurement of break-out noise of mufflers, *SAE Conference, SIAT 2007*, SAE Paper 2007-26-040, ARAI, Pune, India, 501–508, (2007).

[59] Cummings, A., Chang, I.-J., and Astley, R. J. Sound transmission at low frequencies through the walls of distorted circular ducts, *Journal of Sound and Vibration*, **97**, 261–286, (1984).

[60] Munjal, M. L., Gowtham, G. S. H., Venkatesham, B., and Harikrishna Reddy, H. Prediction of breakout noise from an elliptical duct of finite length, *Noise Control Engineering Journal*, **58** (3), 319–327, (2010).

[61] Venkatesham, B., Pathak, A. G., and Munjal, M. L. A one-dimensional model for prediction of breakout noise from a finite rectangular duct with different acoustic boundary conditions, *International Journal of Acoustics and Vibration*, **12** (3), 91–98, (2007).

[62] Dokumaci, E. An approximate dispersion equation for sound waves in a narrow pipe with ambient gradients, *Journal of Sound and Vibration*, **240** (4), 637–646, (2001).

[63] Allam, S. and Abom, M. Acoustic modelling and testing of diesel particulate filters, *Journal of Sound and Vibration*, **288** (1–2), 255–273, (2005).

[64] Allam, S. and Abom, M. Sound propagation in an array of narrow porous channels with application to diesel particulate filters, *Journal of Sound and Vibration*, **291** (4), 882–901, (2006).

[65] Keefe, D. H. Acoustical wave propagation in cylindrical ducts: Transmission line parameter approximations for isothermal and non-isothermal boundary conditions, *Journal of the Acoustical Society of America*, **75** (1), 58–62, (1984).

[66] Munjal, M. L. and Mukherjee, N. K. 1-D acoustic analysis of axial-inlet transverse-outlet air cleaners of rectangular and circular cross-section, *International Journal of Acoustics and Vibration*, **15** (2), 55–64, (2010).

[67] Munjal, M. L. and Mukherjee, N. K. Plane wave analysis of rectangular, axial-inlet, axial-outlet and transverse-inlet transverse-outlet air cleaners, *Noise Control Engineering Journal*, **16** (5), 447–463, (2011).

[68] Knutsson, M., Bodén, H., and Nadampalli, R. V. Experimental investigation of the acoustic effect of non-rigid walls in I.C. Engine intake systems, *Proceedings of the Thirteenth International Congress on Sound and Vibration* (ICSV13), Vienna, Austria, (2006).

[69] Qi, D. and Uesaka, T. Numerical experiments on paper-fluid interaction-permeability of three-dimensional anisotropic fibre network, *Journal of Material Science*, **31**, 4865–4870, (1996).

[70] Elnady, T., Elsadany, S., and Abom, M. Flow and pressure drop calculation using two-ports, *Journal of Vibration and Acoustics*, **133**, 041016, (2011).